p-ISSN 2089 – 0133 e-ISSN 2477-6416
URL : https://jurnal.uns.ac.id/ijap/article/view/73616

Indonesian Journal of Applied Physics (IJAP) Vol. 14 No. 2 page 399
DOI : https://doi.org/10.13057/ijap.v14i2.73616

LITERATURE REVIEW−EFFECT OF ADDITIVES AND POST-TREATMENTS ON CORROSION RESISTANCE AND MECHANICAL PROPERTIES OF PLASMA ELECTROLYTIC OXIDATION PRODUCTS IN MAGNESIUM AND TITANIUM

Sri Rahmadani, Anawati Anawati*
[1]Departemen Fisika, Fakultas Matematika dan Ilmu Pengetahuan Alam, Universitas Indonesia, Depok, Indonesia
*anawati@sci.ui.ac.id

Received 10-05-2023, Revised 19-04-2024, Accepted 13-09-2024,
Available Online 13-09-2024, Published Regularly October 2024

ABSTRACT

Plasma Electrolytic Oxidation (PEO) is a method of converting metal surfaces into an oxide layer with the help of plasma to improve the surface mechanical properties and corrosion resistance of metals. A PEO layer of about 10-50 μm is obtained quickly from 1 second-10 minutes at a voltage range of 150-500 V with AC or DC mode. Characteristics of the outer layer of PEO have pores and cracks, while the inner layer is relatively denser. Cracks and pores reduce the corrosion resistance and mechanical properties of the coating. In this study, a literature search was carried out on the effect of adding additives and post-treatment on the characteristics of PEO coatings grown on magnesium (Mg) and titanium (Ti) metals for biomedical applications. Mg and Ti metals have opposite chemical properties; Mg is a reactive metal, while Ti is an inert metal. Comparing the behavior of the PEO process and the coating produced by the two different metals is absorbing and necessary to understand the fundamentals of the PEO process. The results of a literature search show that the addition of additives increases the growth rate of the coating so that the coating is thicker and more wear resistant. The hardness of the coating also increases due to the additive particles trapped in the oxide layer filling the micro pores so that the surface becomes denser and more homogeneous. Therefore, corrosion resistance also increases, as indicated by a decrease in corrosion current as measured by the polarization test and an increase in the impedance modulus as measured by the electrochemical impedance test (EIS). Among the additive particles, SiO_2 is preferentially used as it gives significant improvement in both mechanical and corrosion properties of PEO coatings. Post treatment is necessary to seal defects in the coatings. The interesting method is alkali treatment considering its simplicity method and improvement in both corrosion resistance and bioactivity.

Keywords: Implant; post treatment; plasma electrolytic oxidation; silicon dioxide

Cite this as: Rahmadani, S., & Anawati. 2024. Literature Review−Effect of Additives and Post-Treatments on Corrosion Resistance and Mechanical Properties of Plasma Electrolytic Oxidation Products in Magnesium and Titanium. *IJAP: Indonesian Journal of Applied Physics, 14*(2), 399-416. doi: https://doi.org/10.13057/ijap.v14i2.73616

INTRODUCTION

The PEO coating method is an electrochemical process at high voltage that produces a ceramic oxide layer on magnesium (Mg), titanium (Ti), aluminium (Al), zirconium (Zr) and their alloys [1]. PEO has many advantages over other coating techniques, such as excellent adhesion properties of the oxide layer to the substrate, simple process, environmental friendliness and relatively low cost. Effective parameters affecting PEO coatings' microstructural characteristics are current/voltage density, processing time, electrolyte type and composition, and temperature [2]. The electrolytes used in PEO can be silicates, aluminates and phosphates. The three electrolyte salts are environmentally friendly. Among the three, the phosphate electrolyte produces the predominant crystalline phase, which makes it harder and corrosion-resistant [3]. The composition of the PEO coating depends on the type of substrate and the composition of the solution used [4]. PEO coatings are expected to have biocompatibility, osseointegration with bone tissue, good corrosion resistance, and appropriate mechanical properties for biomedical applications. Generally, there are two types of implants, permanent implants and temporal (temporary) implants [5]. Examples of the use of permanent implants are prostheses and dental implants. While temporal implants are currently being developed using magnesium-based materials and alloys, iron, zinc, etc. Examples of the use of temporal implants are surgical staples, fixation plates in fracture repair, and stents [6].

The problems still encountered in the PEO coating are high porosity and the appearance of cracks which can reduce the mechanical properties and corrosion resistance [7]. Efforts can be made to optimise electrical parameters, add additives, and post-treatment of the PEO layer. The additives used for biomaterials are Ag, CeO_2, hydroxyapatite (HA), TiO_2, SiC, ZrO_2, Si_3N_4, Al_2O_3, and SiO_2 [8]. Adding additives can reduce the pore size and prevent the appearance of micro-cracks [9]. As reported by Nasiri et al., [7], the addition of SiC particles reduced the porosity of the PEO layer from 22.45% to 18.17%, and the hardness value increased from 280 HV to 410 HV. The coefficient of friction is lower and more stable, thereby increasing the wear resistance of the coating. The post-treatment method is another effective step that can reduce the pore diameter and cracks in the PEO layer [10]. This treatment can increase the corrosion resistance of the coating due to a more homogeneous surface and free of cracks. The formation of a new layer on the PEO layer after post-treatment can also trigger the ability to form new, homogeneous apatite so that bioactivity increases [11]. Therefore, this scientific review will discuss the effect of adding additives and post-treatment on the morphology and composition of the PEO layer.

METHOD

Characteristics of Magnesium and Titanium Metals

Magnesium has superior properties, including its low density (1.35-1.85 g/cm^3), strong, biocompatible, biodegradable, and non-toxic in the body [12]–[14]. However, Mg metal has a relatively fast degradation rate, limiting its more comprehensive application as an implant material [14]. The high corrosion rate causes a high rate of release of hydrogen gas and a decrease in the mechanical properties of the implant before it recovers [15], [16]. Titanium can osteogenesis [17], is lighter with a density value of 1.74 g/cm^3, has a high melting point of around 1660 ºC, increased strength of about 210-1380 MPa, and high biocompatibility [18], [19]. Commercial pure titanium (CP-Ti) has a low elastic modulus value of 105 GPa close to human bone 10-30 GPa compared to alloys of Ti-6Al-4V, Co-Cr, and Stainless steel (ASTM F67) as shown in Table 1 and Table 2.

Table 1. The physical and mechanical properties for metal implants are different compared to natural bone [5].

Material	**Density (g/cm³)**	**Elongation (GPa)**	***Compre-ssive strength* (MPa)**	***Fracture toughness* (MPa.m$^{1/2}$)**
Natural bone	1.8-2.1	3-20	130-180	3-6
Mg	1.74-2.0	41-45	65-100	15-40
Ti	4.4-4.5	110-117	758-1117	55-115
Stainless steel	7.9-8.1	189-205	170-310	50-200
Co-Cr	8.3-9.2	230	450-1000	-
Synthetic HA	3.1	73-117	600	0.7

Metals' protective oxide layer (TiO_2) can increase stable corrosion resistance in human body fluids [13]. Implant materials in the human body must have high bioactivity and osseointegration properties. This is so that the implant can stimulate the growth of new bone tissue. In addition, implant materials must have high corrosion resistance due to being in an aggressive environment and better mechanical and wear properties [12], [20], [21].

Table 2. The physical and mechanical properties of Mg and Ti metal [12].

Material properties	**Mg**	**Ti**
Tensile strength (MPa)	152	345
Yield strength (MPa)	80	275
Melting point (°C)	650	1660
Density (g/cm³)	1,74	4,5
Thermal conductivity (W/mK)	156	16,4
Modulus elasticity (GPa)	45	105

PEO Coating Formation Mechanism

PEO is an electrochemical coating to decompose the metal surface layer into a ceramic oxide layer with the help of plasma excitation at high voltage [12]. The PEO layer has the characteristics of pores and micro-cracks [22]. The PEO process can use various current source modes, including AC source, DC source, unipolar, and bipolar. Variations of the current source mode can modify the surface of the resulting PEO layer [23]. Usually, the voltage applied to the PEO process is between 95 V and 750 V [20]. Electrical conditions with AC power sources produce coatings with superior quality (denser and harder) compared to DC power sources. However, there are obstacles to observing the discharge phenomenon in the PEO process with an AC power source [24]. In general, the schematic of the PEO process circuit can be seen in Figure 1. The substrate is placed as the anode (working electrode), which is connected to the power supply. Meanwhile, the cathode as a counter electrode uses an inert metal (platinum or graphite). Densities and current voltages commonly applied to PEO processes are in the range of 1.5-15 A/dm^2 and 400-500 V for Mg alloy substrates [25], 6-20 A/dm^2 and 200-500 V for Ti alloy substrates [26], and 10-60 A/dm^2 and 200-400 V for Al alloys [27]. Another effective parameter affecting coating is time in the range of 15-60 minutes [28]. The electrolytes commonly used in the PEO process are phosphate, silicate, and aluminate-based electrolytes.

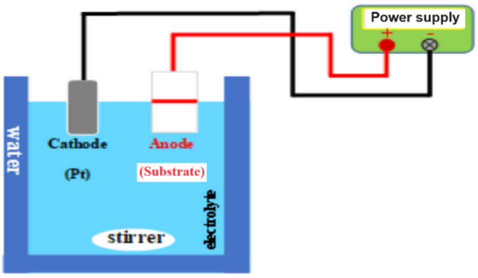

Figure 1. PEO process tool set schematic

The coating formation mechanism in the PEO process goes through several stages, as illustrated in Figure 2. In the first stage, a rapid increase in stress occurs, a conventional anodizing process characterized by forming a thin passive layer. During the formation of the barrier layer, the voltage increases drastically until it reaches the breakdown voltage, and leakage of the dielectric layer occurs—a small white, smooth, and homogeneous plasma splash forms on the surface at this stage. The sparks are distinct in forming the PEO layer [24]. In the second stage, the growth rate of the oxide film becomes reduced as the increase in stress slows down. In the third stage, the plasma spark becomes larger and turns yellow after reaching a constant voltage, and the slope becomes gentler. An orange or intense micro-discharge plasma will appear in the last stage. Voltage fluctuates with PEO processing time [29].

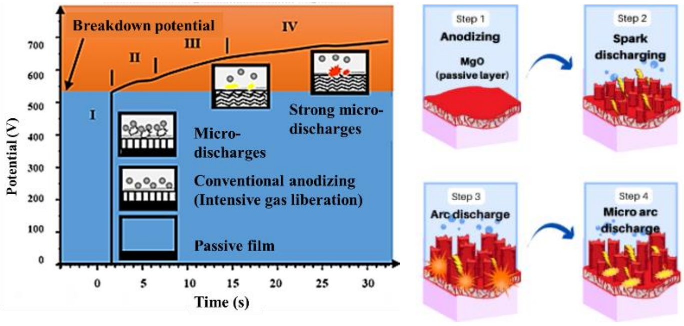

Figure 2. PEO layer formation mechanism

Plasma has several characteristics, including the temperature at the centre of the plasma is higher than the surrounding temperature, has a temperature between 4000-1200 K, an electron density between 1015-1018 cm^3, and the composition of the plasma consists of substances (substrate, coating and electrolyte) [30]. The evolution of distribution and release intensity about the processing time for PEO of magnesium alloy AZ31 in silicate electrolyte was reported by [31]. The longer the PEO time, the bigger and brighter the plasma will be as a measure of intensity.

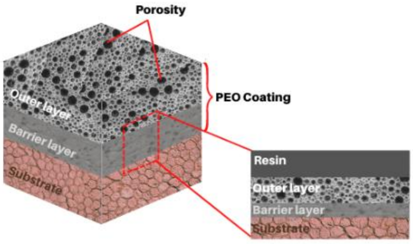

Figure 3. Schematic morphology of PEO layer cross-section

Figure 3 shows the characteristics of the PEO layer, which consists of a porous outer layer, a denser inner layer, and a barrier layer. Pores are formed due to the release of gas trapped in the coating and plasma release channels during the PEO process [12], [32], [33]. The barrier layer is denser, while the inner and outer layers have pores and cracks due to solidification and thermal expansion.

Effect of Current/Voltage Density on PEO Coating Characteristics

The current density is a parameter that affects the microstructure and properties of the PEO layer. Research conducted by Zhuang et al. [34] explained the effect of current density on the PEO AZ31 Mg process in phosphate-based electrolytes. The current density variation applied is 5-20 A/dm^2. The results of this study describe the characteristics of the microstructure, corrosion resistance, and wear resistance which are different for each variation of current density. The layer becomes thicker as the current density increases because more energy induces a reaction on the substrate surface to form a PEO layer quickly. In addition, the PEO current density also affects corrosion resistance, especially the coating formed at a current density of 10 A/dm^2 which is the most superior to other current density variations. Likewise, the wear resistance of the coating is better due to the denser layer structure. These results are similar to those reported in studies [25], [28], [35].

Table 3. Study of the effect of current/voltage density on the PEO layer

Substrate	PEO parameter			Characteristics of coating	Ref.
	Electrolyte	Current parameter (A.dm^{-2})	Time (minutes)	Morphology/porosity/*crack*/thickness	
AZ31 Mg	10 g/l Na_2SiO_3 + 2 g/l KOH + 2,5 g/l K_2ZrF_6	i = 5, 10, 15, and 20	15	Thickness 4.7–14.1 µm, The pore diameter increases, and the number of pores decreases. Crack on the coating surface. Optimum at current density 10 A.dm^{-2}.	[34]
AZ31 Mg	2 g/l $NaAlO_2$ + 2 g/l Na_2SiO_3 + 1,5 g/l KOH	i = 1,15 and 2,3	20	Porosity (22.45% to 23.17%) and the pore size increases (7.57 to 11.32 µm) with increasing current density.	[7]
AM50 Mg	10 g/l Na_2SiO_3 + 10 g/l KOH	i = 1,5, 7,5, and 15	15	Thickness 16–28 µm, pore size increases (1–8 µm), and porosity decreases. Crack in the resulting layer current density 7.5 and 15 A.dm^{-2}.	[25]
AZ31 Mg	0,5 M Na_3PO_4	i = 6, 8, and 10	3	Thickness 14.3–50.4 µm, the smallest porosity, and the highest current density (53.3%) is produced at a current density 8 A.dm^{-2} with a layer thickness 47.6 µm.	[42]
AZ31 Mg	12 g/l $Na_3PO_4.12H_2O$	i = 2,5, 5, 10, and 15	10	Thickness 7.29–13.85 µm, microcrack, roughness increases, and the current density is linear with the pore size.	[43]
AM50 Mg	10 g/l Na_3PO_4 + 1 g/l KOH + 5 g/l Clay	i = 3, 6, and 12	20	Thickness 31–65 µm, 11.1–12 µm pore size, surface cracks for all magnitudes of current density, and reduced porosity (17.6 to 9.9 %).	[44]

PEO, with a short time, produces a relatively homogeneous distributed layer of micropores. The pore number decreases as the coating time increases, but the pore size increases [36]. However, if the time is longer, the large pores will be filled internally because the PEO process produces micro-discharges [37]. The layer formed on the surface results from the melting and solidification of the plasma [38]. The pore diameter on the surface will increase with the time for oxidation [39]. The increase in PEO time contributes to the thickness and hardness of the coating. The PEO coating on AZ31 with current density variations of 500 $A.m^{-2}$, 700 $A.m^{-2}$, up to 900 $A.m^{-2}$ produces a coating with a hardness which is about four times greater (292-301 HV) than the substrate hardness (79 HV) [28]. This is due to the formation of the coating's $Mg_3(PO_4)_2$ and MgO crystalline phases. However, there was an increase in the corrosion current density, and the capacitive loop diameter decreased after 15-20 minutes of PEO due to the formation of large size pores and the presence of micro-cracks so that the corrosive solution could easily penetrate the barrier layer. Other studies also reported similar results [40], [41]. Table 3 describes several studies that reported the effect of the current/voltage density on the PEO layer. A PEO layer of about 10-50 µm is obtained quickly between 1 second to 10 minutes of processing at a voltage range of 150-500 V.

Effect of Electrolyte Composition and Concentration on PEO Coating Characteristics

The type and concentration of electrolyte can affect the morphological properties of the PEO layer. Solutions that can be used for the PEO process on magnesium substrates include electrolytes based on silicates, aluminates, and phosphates [41], [45]–[47]. Yagi et al. [48] modified the surface of the PEO layer on the magnesium alloy ACM522 series with a phosphate-based electrolyte; the PEO layer formed consisted of a monoclinic crystalline $Mg_3(PO_4)_2$ phase. Liang et al. [49] compared the PEO process on AM50 Mg alloy in two different types of electrolytes, namely silicates and phosphates. The PEO layer with silicate-based electrolyte has finer pores and thinner thickness than phosphate-based electrolyte. The main phases for phosphate-based PEO coatings are $Mg_3(PO_4)_2$ and Mg_2SiO_4 for coatings with silicate-based electrolytes. The silicate-based PEO coating has better corrosion resistance because the coating is denser and more substantial. Similar results were reported by Li et al. [50] on Al alloy substrates and Yang et al. [50] on carbon steel substrates.

Hidayati et al. [51] identified a layer of PEO on top of an AZ31 Mg alloy with a phosphate-based electrolyte for 3 minutes at a current density of 400 $A.m^{-2}$, resulting in a layer with a crystalline phase of $Mg_3(PO_4)_2$ and the presence of an amorphous MgO phase and $Mg(OH)_2$. The composition of the PEO layer on the Mg alloy consists of MgO, $MgAl_2O_4$, Mg_2SiO_4, and $Mg_3(PO_4)_2$ depending on the type of electrolyte and type of substrate [22], [36]–[38], [52], [53]. Aliasghari et al. [26] reported coating PEO on Ti substrates with a phosphate/silicate-based electrolyte. The current density is 500 $mA.cm^{-2}$, the frequency is 50 Hz, and the duty cycle is 50% for 900 seconds. The phase formed on the PEO-Ti layer consists of anatase, rutile, amorphous silica, and Ti_2O_5. The layer formed is about 40 to 50 µm thick with a high porosity surface. The outer layer is relatively thicker than the inner layer. Silica was detected more on the outside, and the inside was rich in titania. The current density of the titanium substrate is in the range of 300-900 $mA.cm^{-2}$.

The Effect of Additives on the Characteristics of the PEO Coating

Further research studied the effect of particles added to the PEO electrolyte on the characteristics of the oxide layer as shown in Figure 4. The deposition of microparticles on the surface of the coating has a positive impact on the wear resistance of the coating [54]. Many modifications to the PEO process have been made to increase the corrosion resistance of coatings by adding different particles in the electrolyte. The results showed an increase in the corrosion resistance and wear resistance of the PEO layer with added additives in the electrolyte. Several types of particles added to the PEO process electrolyte are GO, graphite, K_2TiF_6, HAp, TiO_2, SiC, MoS_2, ZrO_2, Al_2O_3, CeO_2, Si_3N_4, and SiO_2 [8], [55]–[58]. Studies on the effect of adding additives to the PEO electrolyte on the corrosion behavior of the PEO Mg and Ti layers are presented in Table 4 and Table 5. Based on these studies it is clear that the PEO Mg and Ti processes can be carried out with different electrical parameters and additives.

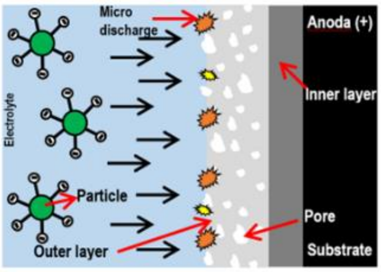

Figure 4. Schematic of addition of particles in the PEO process

Table 4. Study of the effect of the addition of additives on the corrosion behaviour of the PEO Mg coating

Substrate	**Electrolyte**	**No Additives**	**Additives**		**Ref.**
		E_{corr} (V), i_{corr} (A/cm^2)	**Additives type**	**E_{corr} (V),i_{corr} (A/cm^2)**	
AM50	1 g/l KOH 20 g/l Na_3PO_4	E_{cor}= -1,59 i_{corr}= 1.2x10^{-7}	5 g/l SiO_2	E_{cor}= -1.55 i_{corr}= 2.4x10^{-7}	[8]
AZ91D	Na_2SiO $NaAlO_2$	E_{cor}= -1.46 i_{corr}= 9.91×10^{-9}	4 g/l SiC	E_{cor}= -1.37 i_{corr}= 775×10^{-9}	[64]
AZ31	2 g/l $NaAlO_2$ 2 g/l Na_2SiO_3 1,5 g/l KOH	E_{cor}= -1.48 i_{corr}= 1.84x10^{-6}	5 g/l SiC	E_{cor}= -1.42 i_{corr}= 1.26x10^{-6}	[7]
AZ91	50 g/l Na_5P3O_{10} 50 g/l Na_2SiO_3 40 g/l NaOH	E_{cor}= -1.7 i_{corr}= 2x10^{-6}	3 g/l GNP	E_{cor}=-1.72 i_{corr}= 6.0x10^{-7}	[60]
Mg-1%Ca	2 g/l KOH 10 g/l $NaAlO_2$	E_{cor}= -1.2 i_{corr}= 6.8x10^{-6}	4 g/l TiO_2	E_{cor}= -1.38 i_{corr}= 0.15x10^{-6}	[66]

Zhang et al., [59] have reported the effect of adding GO additive to the silicate-based PEO main electrolyte with various compositions of GO-5, GO-10, G-20, and GO-40 ml/L. The addition of additives produces a denser and more homogeneous layer. The percentage of porosity of the GO-20 additive sample decreased five times that of the sample without additives. Most of the pores on the surface of the PEO layer are filled by molten oxide from the discharge channels. The GO-40 additive sample experienced an increase in the percentage of porosity to 2.3% from the GO-20 sample (1.2%). The highest microhardness value was obtained in the GO-20 sample (572.9 $HV_{0.3kg}$) due to the denser microstructure and increased phase containing silicate. No new phase formation occurred but an increase in the diffraction peak intensity of the main component of the PEO layer was detected with the addition of GO additives. The addition of additives encourages the formation of more MgO and Mg_2SiO_4 phases. There was an increase in corrosion resistance of up to three orders in the GO-20 sample with polarization resistance values increasing up to two times compared to the sample without additives. The efficiency of protection against corrosion increases due to the incorporation effect of embedded GO reducing the porosity of the PEO layer. Similar results were reported in [60] with the addition of graphite additives which can increase corrosion resistance marked by a decrease in the corrosion current density of up to two orders. Graphite particles close the pores in the PEO layer so that the surface becomes more homogeneous and denser which acts as a barrier layer when in a corrosive environment.

Table 5. Study of the effect of the addition of additives on the corrosion behaviour of the PEO Ti coating

Substrate	**Electrolyte**	**No Additives**	**Additives**		**Ref.**
		Corrosion properties (E_{corr} (V), i_{corr} (A/cm^2))	**Additives type**	**Corrosion properties (E_{corr} (V), i_{corr} (A/cm^2))**	
Pure Ti Grade 2	5 g/l $Na_3PO_4.12H_2O$ 3 g/l KOH 1,03 g/l $Ca_3(PO_4)_2$	$E_{corr} = +0.16$ $i_{corr} = 0.14x10^{-7}$	1, 3, dan 5 g/l ZrO_2	$E_{corr} = +0.05$ $i_{corr} = 0.12x10^{-7}$	[70]
Pure Ti Grade 2	8 g/l $Na_3PO_4 \cdot 12H_2O$	$E_{corr} = -0.08$ $i_{corr} = 11x10^{-9}$	1, 5, 3, and 4.5 g/l α-Al_2O_3	$E_{corr} = -0.05$ $i_{corr} = 22.2x10^{-9}$	[71]
CP α-Ti	20 g/l $Na_3PO_4.12H_2O$ 4 g/l NaOH	$E_{corr} = +0.11$ $i_{corr} = 7.46x10^{-8}$	5,10, and 15 g/l ZnO	$E_{corr} = +0.02$ $i_{corr} = 0.77x10^{-8}$	[72]
Pure Ti Grade 2	5 g/l $Na_3PO_4.12H_2O$ 3 g/l KOH 1 g/l $Ca_3(PO_4)_2$	$E_{corr} = +0.16$ $i_{corr} = 0.14x10^{-6}$	1, 3, and 5 g/l TiO_2	$E_{corr} = +0.13$ $i_{corr} = 0.06x10^{-6}$	[73]
CP-Ti	15 g/l $NaSiO_3$ 2 g/l Na_3PO_4 3 g/l KOH	$E_{corr} = -0.41$ $i_{corr} = 2.59x10^{-7}$	3, 6, and 10 g/l Al_2O_3 TEA	$E_{corr} = -0.17$ $i_{corr} = 7.76x10^{-9}$	[74]

Rahmati et al. [61] identified the PEO layer on Mg AZ31 in a silica-based solution by adding the additive K_2TiF_6 in various concentrations. PEO coating with additives produces thicker layers with reduced pore diameter and cracks. The optimum additive concentration with the lowest porosity percentage (13.04%) was 5 g/l with a current density of 15.86 mS.cm^{-1}. As the concentration of K_2TiF_6 increases, the layer formed becomes more porous. The PEO layer without additives contains MgO, SiO_2 (amorphous), Mg_2SiO_4, and $MgSiO_3$ phases. A new phase was formed in the PEO layer by adding the additive K_2TiF_6, namely the MgF_2 and TiO_2 phases (crystalline and amorphous) the greater the concentration of the additive, the more amorphous phase formation. TiO_2 fills micro pores making it denser and thicker-silicate ions in the main solution form amorphous SiO_2, contributing to a partial sealing effect. The highest corrosion resistance was achieved with a concentration of 5 g/l K_2TiF_6 due to a dense inner layer of MgF_2. The coating corrosion performance was increased, marked by the widening of the capacitive up to two loops caused by the sealing effect of the outer layer micro-pores by the incorporation of TiO_2 particles and the formation of SiO_2. Similar to that reported by [53] PEO Mg AZ31 with the addition of sodium tetraborate and [62] with the addition of K_2ZrF_6.

HAp added to a silicate-based PEO Mg AZ80 solution contributed to the growth process of the PEO layer [63]. The diffraction results showed the presence of HA particles in the PEO layer, so the polarization resistance value doubled with the addition of HA in the electrolyte. Self-sealing bioceramic coating with the addition of HA can increase the bioactivity properties of the coating due to its chemical and biological similarities with natural bone tissue.

Nasiri et al. [7] reported the research results by adding SiC nanoparticles in the electrolyte to produce a nanocomposite layer with a more stable friction coefficient than without SiC additives. Yu et al. [1] reported PEO on Mg AZ31 in silicate and phosphate-based electrolytes with SiC nanoparticles (~100–2000 nm) after dilution to prevent particle agglomeration during the PEO process. This study showed an increase in the growth rate of the coating without and with the addition of SiC nanoparticles, from 21 µm/minute to 37 µm/minute. In addition, corrosion resistance increases based on a decrease in the current density of corrosion from $2x10^{-6}$ $A.cm^{-2}$ to $9.25x10^{-7}$ $A.cm^{-2}$. The wear resistance of the coating is closely related to the surface hardness. SiC is a very hard particle (3000 HV) distributed on the oxide layer's surface [1]. Nano-sized ceramic particles trapped in the coating are protective in increasing wear resistance. In addition, the addition of SiC nanoparticle additives in the electrolyte increases the hardness value of the coating compared to no additives with the same process parameters. SiC nanoparticles fill the pores or are trapped in the oxide layer, increasing the hardness value of the layer [64].

The addition of additives in the PEO electrolyte also affects the corrosion behaviour of the coating. The effect of SiC nanoparticles incorporated in the pores is a barrier to the transfer of corrosive Cl ions and suppresses the corrosion current density [64]. The low electrical conductivity of SiC nanoparticles acts as a barrier in electron transfer. The amount of Mg is the most dominant compared to other elements, especially element C which comes from SiC nanoparticles. The same thing was also observed in the research of Mohedano et al. [65]. The PEO process with phosphate-based electrolyte on Mg AM50 resulted in a decrease in pore size and density on the surface by increasing the concentration of additive particles from 2 g/l to 10 g/ l (ZrO_2, α-Al_2O_3, and CeO_2). A better additive added in the formation of PEO coating is CeO_2, with long-term corrosion performance. Adding additives to the PEO solution can increase the hardness value of the PEO layer, as shown in Figure 5.

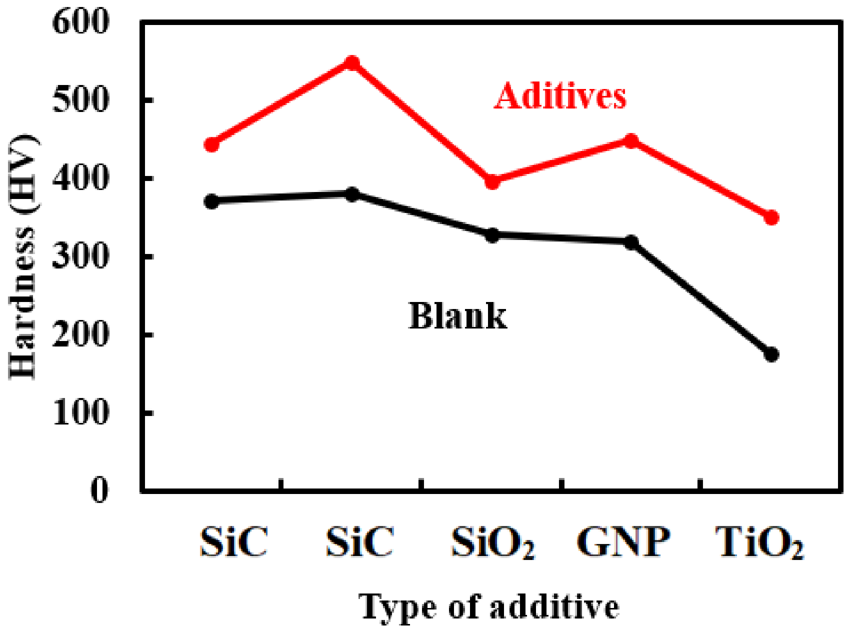

Figure 5. Effect of additive on the hardness value of the PEO Mg coating [7], [8], [60], [64], [66].

The PEO process on Ti grade 2 was reported by Malinovschi et al. [67] using a DC source of 0.36 $A.cm^{-2}$ and electrolyte $NaAlO_2$ with various concentrations from 10-20 g/l. The dominant crystalline phases formed were α-Al_2O_3 and γ-Al_2O_3. Other phases with minor concentrations are $TiAl_2O_5$ and $Na_2Ti_4O_9$. The increase in electrolyte concentration and the length of time for oxidation increased the thickness of the PEO layer. The thickest layer has better wear resistance. In addition, the addition of electrolyte concentration can also reduce the size of the micropores formed on the surface of the coating, thereby increasing corrosion resistance. Sarbishei et al. [68] also reported PEO results on Ti substrates in silicate-based electrolytes added to alumina nanoparticles. Alumina particles were found to precipitate to fill the pores on the surface of the PEO results, thereby reducing the amount of porosity (15.2%). The PEO coating can increase titanium's corrosion resistance by up to 10 times. These results are similar to the study by Vasilyeva et al. [69]; the coating surface becomes more homogeneous after adding acetonitrile to the primary electrolyte and increases adhesion to the substrate.

SiO_2 is widely chosen as an additive in PEO electrolytes because it produces a functional, corrosion-resistant, wear-resistant coating and has good biodegradability [75]. Based on the analysis results in Table 6, it can be confirmed that the optimum concentration of SiO_2 particles to increase corrosion behaviour is up to two orders of magnitude in magnesium alloys, namely in the range of 2 g/l to 5 g/l [76].

Table 6. Study of the effect of adding SiO_2 additives on the morphology and corrosion behavior of PEO coating

Substrate	Electrolyte + Aditives	Phase	Corrosion properties (E_{corr} (V), i_{corr} (A/cm^2))	Result	Ref.
AM50	1 g/l KOH 20 g/l Na_3PO_4 + 5 g/l SiO_2	MgO SiO_2	E_{corr} = -1.566 i_{corr} = 1.9x10^{-7}	The number of pores increases Shrinking pore size	[8]
Pure Mg 9995A	7 g/l $Na_2HPO_4 \cdot 12H_2O$ 3 g/l KOH + 3 g/l SiO_2	MgO $Mg_3(PO_4)_2$ Mg_2SiO_4	E_{corr} = -1.44 i_{corr} = 8.18x10^{-4}	n-SiO_2 was detected in the PEO layer	[54]
MA8	15 g/l NaF 15 g/l Na_2SiO_3 + 4 g/l SiO_2	MgO Mg_2SiO_4	E_{corr} = -1.50 i_{corr} = 8.20x10^{-8}	Porosity is reduced Thickness increase	[76]
MA8	NaF Na_2SiO_3 + 0.1 g/l SiO_2	MgO Mg_2SiO_4	E_{corr} = -1.42 i_{corr} = 3.3x10^{-7}	More nodular (homogeneous) surface	[77]
AM50	1 g/l KOH 20 g/l Na_3PO_4 + 5 g/l SiO_2	SiO_2	-	Wear resistance increases Shrinking pore size	[78]
CP-Ti	10 g/l Na_3PO_4 + 4 g/l SiO_2	Anatase	-	SiO_2 nanoparticles are homogeneously distributed	[79]

PEO Coating Post Treatment Method

Several methods that have been widely used as alternatives to improve the properties of PEO coatings include hydrothermal [80], sealing treatments (sol-gel, alkali treatment, organic and inorganic coatings) [10], [81]–[87], silane layer [81], [88]–[90], and conversion surface treatment [86], [91].

Tian et al. [80] reported PEO Mg AZ31 in a silicate-based electrolyte by hydrothermal (HT) method as post-treatment. The HT solutions used were 0.1 M Ca-EDTA, KH_2PO_4, and 1 M NaOH. The HA layer formed on top of the PEO layer managed to cover the pores on the surface, thereby increasing the corrosion resistance in the SBF solution based on the PDP test results. The PEO layer has a corrosion potential value that shifts to a relatively negative position (E_{corr}= −1.640 V). In contrast, the value of the corrosion current density decreases significantly (i_{corr}= 4.74x10^{-7} A.cm^{-2}) about two orders compared to the substrate (E_{corr}= −1.508 V, i_{corr}= 1.4x10^{-5} A.cm^{-2}). The PEO-HT coating presented a more positive corrosion potential (Ecorr = −1.234 V) and a much lower corrosion current density (i_{corr}= 2.1x10^{-9} A.cm^{-2}), about four times the substrates. PEO/HT coating also has good bioactivity and, biocompatibility, flexible fabrication. It is suitable for adhesion and proliferation, making it promising in surface modification of biodegradable magnesium-based implants for orthopaedic applications.

The sealing treatment method was reported by Van Phuong et al. [10], with sealing results in two different solutions (cerium and phosphate) on the PEO Mg layer. PEO electrolyte composition consisted of 0.7 M NaOH, 0.1 M NaF, 0.1 M Na_3PO_4 and 0.1 M Na_2SiO_3 for 5 minutes. The first sealing treatment was in a 0.023 M $Ce(NO_3)_6H_2O$ solution and 0.25 M H_2O at 25ºC. Second sealing in 0.1 M NaH_2PO_4 solution at 90ºC. Both were carried out for 20 minutes each. The results of this treatment succeeded in closing the pores and reducing cracks in the PEO layer. The first sealing treatment stored the cerium compound in the PEO layer, but some of the layers would dissolve if soaked longer. The combination of double sealing can significantly increase the corrosion resistance of the PEO coating. After the first sealing treatment and a second sealing in a phosphate solution, it can change CeO into a more stable $CePO_4$.

The results of a similar study were reported by Mingo et al. [81], identifying the characteristics of the PEO Mg AZ91 layer by the post-treatment sealing method in three different solutions (serum, stained, and ODP acid). Compounds formed after sealing consists of CeO2, MgSn $(OH)_6$, and SnO. Even though this treatment did not completely cover the surface of the PEO layer, it still filled in the pores and cracks, thereby slightly increasing the corrosion resistance. Sealing in ODP acid solution gave the best results due to the increased hydrophobicity of the ODP monolayer.

The sol-gel hybrid method and epoxy coating were reported by Liu et al. [85] on the PEO Mg AM50 coating, which was adequate for closing pores and free from cracks. This is due to an organic/inorganic composite layer which can increase the adhesion strength, corrosion resistance, and wear performance. Fluorine-containing polymers are hydrophobic on the surface of the coating. The epoxy resin distributes the corrosion inhibitor into the pores of the PEO coating. The thickness of the coating will increase with increasing immersion time, although the surface roughness will decrease. These results are similar to those reported by [92], [93].

Alkali treatment is a treatment that can fill the pores of the PEO layer without destroying the bioactivity properties of the layer. In general, this method is used to improve the characteristics of PEO coatings on Mg and Ti alloys so that they can contribute to implant applications. Research reported [94] alkaline treatment using 0.25 M NaOH solution at 80˚C for 90 minutes confirmed the presence of a layer of Mg $(OH)_2$. The sub-microns in the PEO layer can form homogeneous apatite, making it practical for increasing the corrosion resistance and bioactivity of AZ31 alloy. [11] they have also presented the results of an alkaline treatment study with a 3 M NaOH solution at 60˚C for 1 hour on silicate-based PEO Mg. The total Ca/P ratio increased due to the formation of a thick corrosion layer and covered the pores of the PEO layer after the alkali treatment. This step can effectively reduce the pore size and increase the surface homogeneity of PEO Mg layers with spherical or globular morphology. This treatment can increase corrosion resistance, as evidenced by a decrease in the value of the corrosion current density from 1.7×10^{-6} $A.cm^{-2}$ to 4.42×10^{-7} $A.cm^{-2}$. In addition, the alkaline treatment is also a simple treatment compared to plasma spray and sputtering, does not involve high temperatures, and can increase the surface homogeneity of the PEO layer.

CONCLUSION

Based on the results of the literature review, it can be concluded that the process and characteristics of the PEO coating on Mg and Ti are enjoyable to discuss because Mg and Ti have opposite properties, namely Mg is a reactive metal, while Ti is an inert metal. Both metals are used in biomedical implant applications. The problem researchers are still facing with PEO Mg and Ti is irregular cracks and pores, which reduce the coatings' corrosion resistance and mechanical properties. PEO, adding additives, produces a coating with better corrosion and wear resistance. The additive that can potentially be used in the PEO process for biomedical implant applications is SiO_2 because it produces a PEO layer with good wear resistance and is biodegradable. The optimum concentration of SiO_2 particles to increase the corrosion behaviour of the PEO coating is in the range of 2 g/l to 5 g/l. Alkali treatment methods can increase the corrosion resistance of the PEO coating and improve the bioactivity properties of the coating for biomedical applications.

REFERENCES

1 Yu, L., Cao, J., & Cheng, Y. 2015. An improvement of the wear and corrosion resistances of AZ31 magnesium alloy by plasma electrolytic oxidation in a silicate-hexametaphosphate electrolyte with the suspension of SiC nanoparticles. *Surface and Coatings Technology, 276*, 266–278.

2 Wang, Y., et al. 2020. Effect of laser surface remelting pretreatment with different energy density on MAO bioceramic coating. *Surface and Coatings Technology, 393*(January), 125815.

3 Asoh, H., Asakura, K., & Hashimoto, H. 2020. Effect of alcohol addition on the structure and corrosion resistance of plasma electrolytic oxidation films formed on AZ31B magnesium alloy. *RSC Advances, 10*(15), 9026–9036.

4 Fattah-alhosseini, A., Molaei, M., & Babaei, K. 2020. The effects of nano- and micro-particles on properties of plasma electrolytic oxidation (PEO) coatings applied on titanium substrates: A review. *Surfaces and Interfaces, 21*(August), 100659.

5 Tsakiris, V., Tardei, C., & Clicinschi, F. M. 2021. Biodegradable Mg alloys for orthopedic implants – A review. *Journal of Magnesium and Alloys, 9*(6), 1884–1905.

6 Santos-Coquillat, A., Martinez-Campos, E., Sánchez, H. M., Moreno, L., Arrabal, R., Mohedano, M., ... & Matykina, E. 2021. Hybrid functionalized coatings on metallic biomaterials for tissue engineering. *Surface and Coatings Technology*, *422*, 127508..

7 Nasiri Vatan, H., Ebrahimi-Kahrizsangi, R., & Kasiri-Asgarani, M. 2016. Structural, tribological and electrochemical behavior of SiC nanocomposite oxide coatings fabricated by plasma electrolytic oxidation (PEO) on AZ31 magnesium alloy. *Journal of Alloys and Compounds, 683*, 241–255.

8 Lu, X., Blawert, C., Huang, Y., Ovri, H., Zheludkevich, M. L., & Kainer, K. U. 2016. Plasma electrolytic oxidation coatings on Mg alloy with addition of SiO2 particles. *Electrochimica Acta, 187,* 20–33.

9 Shen, M. J., Wang, X. J., & Zhang, M. F. 2012. High-compactness coating grown by plasma electrolytic oxidation on AZ31 magnesium alloy in the solution of silicate-borax. *Applied Surface Science, 259,* 362–366.

10 Van Phuong, N., Fazal, B. R., & Moon, S. 2017. Cerium- and phosphate-based sealing treatments of PEO coated AZ31 Mg alloy. *Surface and Coatings Technology, 309,* 86–95.

11 Narayanan, T. S. N. S., & Lee, M. H. 2016. A simple strategy to modify the porous structure of plasma electrolytic oxidation coatings on magnesium. *RSC Advances, 6*(19), 16100–16114.

12 Chaharmahali, R., Fattah-alhosseini, A., & Babaei, K. 2021. Surface characterization and corrosion behavior of calcium phosphate (Ca-P) base composite layer on Mg and its alloys using plasma electrolytic oxidation (PEO): A review. *Journal of Magnesium and Alloys, 9*(1), 21–40.

13 Klimas, J., Łukaszewicz, A., Szota, M., & Szota, K. 2016. Characteristics of titanium Grade 2 and evaluation of corrosion resistance. *Surface and Coatings Technology, 77*(2), 65–71.

14 Witte, F. (2015). Reprint of: The history of biodegradable magnesium implants: A review. *Acta Biomaterialia, 23*(S), S28–S40.

15 Kraus, T., et al. 2018. The influence of biodegradable magnesium implants on the growth plate. *Acta Biomaterialia, 66*, 109–117.

16 Tian, P., Peng, F., Wang, D., & Liu, X. 2017. Corrosion behavior and cytocompatibility of fluoride-incorporated plasma electrolytic oxidation coating on biodegradable AZ31 alloy. *Regenerative Biomaterials, 4*(1), 1–10.

17 Koçak, A. 2018. Materials science and engineering: Thin film preparation, particle size and thickness analysis experimental report. *Surface and Coatings Technology, February*, 31.

18 Erakovic, S., Janković, A., Veljović, D., Palcevskis, E., Mitrić, M., Stevanović, T., ... & Mišković-Stanković, V. 2013. Corrosion stability and bioactivity in simulated body fluid of silver/hydroxyapatite and silver/hydroxyapatite/lignin coatings on titanium obtained by electrophoretic deposition. *The Journal of physical chemistry B, 117*(6), 1633-1643.

19 Jambagi, S. C., & Malik, V. R. 2021. A review on surface engineering perspective of metallic implants for orthopaedic applications. *JOM, 73*(12), 4349–4364.

20 Sikdar, S., Menezes, P. V., Maccione, R., Jacob, T., & Menezes, P. L. 2021. Plasma electrolytic oxidation (PEO) process—processing, properties, and applications. *Nanomaterials, 11*(6).

21 Wan, P., Tan, L., & Yang, K. 2016. Surface modification on biodegradable magnesium alloys as orthopedic implant materials to improve bio-adaptability: A review. *Journal of Materials Science & Technology, 32*(9), 827–834.

22 Anawati, A., & Gumelar, M. D. 2018. Characterization of coatings formed on AZX magnesium alloys by plasma electrolytic oxidation. *AIP Conference Proceedings, 1964*.

23 Yao, Z. P., Wang, D. L., Xia, Q. X., Zhang, Y. J., Jiang, Z. H., & Wang, F. P. 2012. Effect of PEO power modes on structure and corrosion resistance of ceramic coatings on AZ91D Mg alloy. *Surface Engineering, 28*(2), 96–101.

24 Farshid, S., & Kharaziha, M. 2021. Micro and nano-enabled approaches to improve the performance of plasma electrolytic oxidation coated magnesium alloys. *Journal of Magnesium and Alloys, 9*(5), 1487–1504.

25 Bala Srinivasan, P., Liang, J., Blawert, C., Störmer, M., & Dietzel, W. 2009. Effect of current density on the microstructure and corrosion behaviour of plasma electrolytic oxidation treated AM50 magnesium alloy. *Applied Surface Science, 255*(7), 4212–4218.

26 Aliasghari, S., Skeleton, P., & Thompson, G. E. 2014. Plasma electrolytic oxidation of titanium in a phosphate/silicate electrolyte and tribological performance of the coatings. *Applied Surface Science, 316*(1), 463–476.

27 Wheeler, J. M., Curran, J. A., & Shrestha, S. 2012. Microstructure and multi-scale mechanical behavior of hard anodized and plasma electrolytic oxidation (PEO) coatings on aluminum alloy 5052. *Surface and Coatings Technology, 207*, 480–488.

28 Rahman, F. A. 2021. Karakteristik coating hasil plasma electrolytic oxidation pada paduan magnesium AZ31B: Pengaruh rapat arus dan waktu. *Skripsi*, 80.

29 Tang, H., Wang, M., Zhu, B., & He, L. 2020. Growth process and dielectric breakdown of micro arc oxidation coating on AZ31 Mg alloy pretreated by alkali treatment. *Protection of Metals and Physical Chemistry of Surfaces, 56*(1), 156–163.

30 Hussein, R. 2013. An investigation of ceramic coating growth mechanisms in plasma electrolytic oxidation (PEO) processing.

31 Simchen, F., Sieber, M., Kopp, A., & Lampke, T. 2020. Introduction to plasma electrolytic oxidation—An overview of the process and applications. *Coatings, 10*(7).

32 Bagheri, H., Aliofkhazraei, M., & Nabavi, H. F. 2017. Effect of nanocrystallization on discharge behavior and microstructure of plasma electrolytic oxidation on AZ31B alloy. *Protection of Metals and Physical Chemistry of Surfaces, 53*(6), 1028–1033.

33 Rakoch, A. G., et al. 2020. Plasma electrolytic oxidation of AZ31 and AZ91 magnesium alloys: Comparison of coatings formation mechanism. *Journal of Magnesium and Alloys, 8*(3), 587–600.

34 Zhuang, J. J., Song, R. G., Xiang, N., Xiong, Y., & Hu, Q. 2017. Effect of current density on microstructure and properties of PEO ceramic coatings on magnesium alloy. *Surface Engineering, 33*(10), 744–752.

35 Al Afghani, F., & Anawati, A. 2021. Plasma electrolytic oxidation of zircaloy-4 in a mixed alkaline electrolyte. *Surface and Coatings Technology, 426*.

36 Ma, X., Blawert, C., Höche, D., Kainer, K. U., & Zheludkevich, M. L. 2017. A model describing the growth of a PEO coating on AM50 Mg alloy under constant voltage mode. *Electrochimica Acta*, *251*, 461–474.

37 Duan, H., Yan, C., & Wang, F. 2007. Growth process of plasma electrolytic oxidation films formed on magnesium alloy AZ91D in silicate solution. *Electrochimica Acta*, *52*(15), 5002–5009.

38 Bala Srinivasan, P., Blawert, C., & Dietzel, W. 2008. Effect of plasma electrolytic oxidation treatment on the corrosion and stress corrosion cracking behaviour of AM50 magnesium alloy. *Materials Science and Engineering A*, *494*(1–2), 401–406.

39 Dehnavi, V., Binns, W. J., Noël, J. J., Shoesmith, D. W., & Luan, B. L. 2018. Growth behaviour of low-energy plasma electrolytic oxidation coatings on a magnesium alloy. *Journal of Magnesium and Alloys*, *6*(3), 229–237.

40 Fattah-alhosseini, A., Chaharmahali, R., & Babaei, K. 2020. Effect of particles addition to solution of plasma electrolytic oxidation (PEO) on the properties of PEO coatings formed on magnesium and its alloys: A review. *Journal of Magnesium and Alloys*, *8*(3), 799–818.

41 Toulabifard, A., Rahmati, M., Raeissi, K., & Hakimizad, A. 2020. The effect of electrolytic solution composition on the structure, corrosion, and wear resistance of PEO coatings. *Coatings*.

42 Anawati, A. 2021. Characteristics of magnesium phosphate coatings formed on AZ31 Mg alloy by plasma electrolytic oxidation with improved current efficiency. *SpringerReference*.

43 Hadzima, B., Kajánek, D., Drábiková, J., Březina, M., Buhagiar, J., & Matej, J. (2020). PEO of AZ31 Mg alloy: Effect of electrolyte phosphate content and current density. *Metals*, *10*(1521), 1–23.

44 Rapheal, G. 2016. Effect of current density on the microstructure and corrosion properties of plasma electrolytic oxidation (PEO) coatings on AM50 Mg alloy produced in an electrolyte containing clay additives. *SpringerReference*.

45 Molaei, M., Fattah-Alhosseini, A., & Gashti, S. O. 2018. Sodium aluminate concentration effects on microstructure and corrosion behavior of the plasma electrolytic oxidation coatings on pure titanium. *Metallurgical and Materials Transactions A*, *49*(1), 368–375.

46 Jian Wei, B., Cheng, Y. L., Liu, Y. Y., Zhu, Z. D., & Cheng, Y. L. 2021. Corrosion and wear resistance of AZ31 Mg alloy treated by duplex process of magnetron sputtering and plasma electrolytic oxidation. *Transactions of Nonferrous Metals Society of China*, *31*(8), 2287–2306.

47 Li, Z., Ren, Q., Wang, X., Kuang, Q., Ji, D., Yuan, R., & Jing, X. 2019. Effect of phosphate additive on the morphology and anti-corrosion performance of plasma electrolytic oxidation coatings on magnesium—Lithium alloy. *Corrosion Science*, *157*, 295-304.

48 Yagi, S., Sengoku, A., Kubota, K., & Matsubara, E. 2012. Surface modification of ACM522 magnesium alloy by plasma electrolytic oxidation in phosphate electrolyte. *Corrosion Science*, *57*, 74–80.

49 Liang, J., Srinivasan, P. B., Blawert, C., Störmer, M., & Dietzel, W. 2009. Electrochemical corrosion behaviour of plasma electrolytic oxidation coatings on AM50 magnesium alloy formed in silicate and phosphate-based electrolytes. *Electrochimica Acta*, *54*(14), 3842–3850.

50 Li, J., Cai, H., Xue, X., & Jiang, B. 2010. The outward-inward growth behavior of microarc oxidation coatings in phosphate and silicate solution. *Materials Letters*, *64*(19), 2102–2104.

51 Hidayati, E., & Anawati, A. 2020. Characterization of microstructure and composition of plasma electrolytic oxide film formed on AZ31 Mg alloy. In *Key Engineering Materials* (Vol. 860 KEM, pp. 213–217).

52 Moon, S., Arrabal, R., & Matykina, E. 2015. 3-Dimensional structures of open-pores in PEO films on AZ31 Mg alloy. *Materials Letters*, *161*, 439–441.

53 Sreekanth, D., Rameshbabu, N., & Venkateswarlu, K. 2012. Effect of various additives on morphology and corrosion behavior of ceramic coatings developed on AZ31 magnesium alloy by plasma electrolytic oxidation. *Ceramics International*, *38*(6), 4607–4615.

54 Krishtal, M. M., Ivashin, P. V., Polunin, A. V., & Borgardt, E. D. 2019. The effect of dispersity of silicon dioxide nanoparticles added to electrolyte on the composition and properties of oxide layers formed by plasma electrolytic oxidation on magnesium 9995A. *Materials Letters, 241*, 119–122.

55 Lou, B. S., Lin, Y. Y., Tseng, C. M., Lu, Y. C., Duh, J. G., & Lee, J. W. 2017. Plasma electrolytic oxidation coatings on AZ31 magnesium alloys with Si_3N_4 nanoparticle additives. *Surface and Coatings Technology, 332*, 358–367.

56 Arrabal, R., Matykina, E., Viejo, F., Skeldon, P., Thompson, G. E., & Merino, M. C. 2008. AC plasma electrolytic oxidation of magnesium with zirconia nanoparticles. *Applied Surface Science, 254*(21), 6937–6942.

57 Lou, B. S., Lee, J. W., Tseng, C. M., Lin, Y. Y., & Yen, C. A. 2018. Mechanical property and corrosion resistance evaluation of AZ31 magnesium alloys by plasma electrolytic oxidation treatment: Effect of MoS_2 particle addition. *Surface and Coatings Technology, 350*, 813–822.

58 Mashtalyar, D. V., Imshinetsky, I. M., & Sinebryukhov, S. L. 2017. Formation and properties of composite nanostructured PEO-coatings on metals and alloys. *MATEC Web of Conferences, 129*, 1–5.

59 Zhang, Y., Chen, F., Zhang, Y., & Du, C. 2020. Influence of graphene oxide additive on the tribological and electrochemical corrosion properties of a PEO coating prepared on AZ31 magnesium alloy. *Tribology International, 146*.

60 Pezzato, L., Angelini, V., Brunelli, K., Martini, C., & Dabalà, M. 2018. Tribological and corrosion behavior of PEO coatings with graphite nanoparticles on AZ91 and AZ80 magnesium alloys. *Transactions of Nonferrous Metals Society of China, 28*(2), 259–272.

61 Rahmati, M., Raeissi, K., Toroghinejad, M. R., Hakimizad, A., & Santamaria, M. 2020. The multi-effects of K_2TiF_6 additive on the properties of PEO coatings on AZ31 Mg alloy. *Surface and Coatings Technology, 402*, 1–12.

62 Li, C. Y., Fan, X. L., Cui, L. Y., & Zeng, R. C. 2020. Corrosion resistance and electrical conductivity of a nano ATO-doped MAO/methyltrimethoxysilane composite coating on magnesium alloy AZ31. *Corrosion Science, 168*, 108570.

63 Xiong, Y., Yang, Z., Hu, X., & Song, R. 2019. Bioceramic coating produced on AZ80 magnesium alloy by one-step microarc oxidation process. *Journal of Materials Engineering and Performance, 28*(3), 1691–1699.

64 Wang, S. Y., Si, N. C., Xia, Y. P., & Liu, L. 2015. Influence of nano-SiC on microstructure and property of MAO coating formed on AZ91D magnesium alloy. *Transactions of Nonferrous Metals Society of China, 25*(6), 1926–1934.

65 Mohedano, M., Arrabal, R., Mingo, B., Pardo, A., & Matykina, E. 2018. Role of particle type and concentration on characteristics of PEO coatings on AM50 magnesium alloy. *Surface and Coatings Technology, 334*, 328–335.

66 Daroonparvar, M., Yajid, M. A. M., Yusof, N. M., & Bakhsheshi-Rad, H. R. 2016. Preparation and corrosion resistance of a nanocomposite plasma electrolytic oxidation coating on Mg-1%Ca alloy formed in aluminate electrolyte containing titania nano-additives. *Journal of Alloys and Compounds, 688*, 841–857.

67 Malinovschi, V., Marin, A. H., Ducu, C., Moga, S., Andrei, V., Coaca, E., ... & Lungu, C. P. 2021. Improvement of mechanical and corrosion properties of commercially pure titanium using alumina PEO coatings. *Coatings*, *12*(1), 29.

68 Sarbishei, S., Faghihi Sani, M. A., & Mohammadi, M. R. 2014. Study plasma electrolytic oxidation process and characterization of coatings formed in an alumina nanoparticle suspension. *Vacuum, 108*, 12–19.

69 Vasilyeva, M. S., Rudnev, V. S., & Kuryavyi, V. G. 2019. The effect of acetonitrile additives to tetraborate electrolyte on the composition and morphology of PEO layers on titanium. *Protection of Metals and Physical Chemistry of Surfaces*, *55*(3), 473–480.

70 Molaei, M., Fattah-alhosseini, A., Nouri, M., Mahmoodi, P., & Nourian, A. 2022. Enhancing cytocompatibility, antibacterial activity and corrosion resistance of PEO coatings on titanium using incorporated ZrO_2 nanoparticles. *Surfaces and Interfaces, 30*, 101967.

71 Sharifi, H., Aliofkhazraei, M., Darband, G. B., & Rouhaghdam, A. S. 2016. Characterization of PEO nanocomposite coatings on titanium formed in electrolyte containing atenolol. *Surface and Coatings Technology, 304*, 438–449.

72 Roknian, M., Fattah-alhosseini, A., Gashti, S. O., & Keshavarz, M. K. 2018. Study of the effect of ZnO nanoparticles addition to PEO coatings on pure titanium substrate: Microstructural analysis, antibacterial effect and corrosion behavior of coatings in Ringer's physiological solution. *Journal of Alloys and Compounds, 740*, 330–345.

73 Molaei, M., Fattah-alhosseini, A., Nouri, M., Mahmoodi, P., & Nourian, A. 2022. Incorporating TiO_2 nanoparticles to enhance corrosion resistance, cytocompatibility, and antibacterial properties of PEO ceramic coatings on titanium. *Ceramics International, 48*(14), 21005–21024.

74 Sarbishei, S., Faghihi Sani, M. A., & Mohammadi, M. R. 2016. Effects of alumina nanoparticles concentration on microstructure and corrosion behavior of coatings formed on titanium substrate via PEO process. *Ceramics International, 42*(7), 8789–8797.

75 Molaei, M., Babaei, K., & Fattah-alhosseini, A. 2021. Improving the wear resistance of plasma electrolytic oxidation (PEO) coatings applied on Mg and its alloys under the addition of nano- and micro-sized additives into the electrolytes: A review. *Journal of Magnesium and Alloys, 9*(4), 1164–1186.

76 Gnedenkov, S. V., Sinebryukhov, S. L., Mashtalyar, D. V., Imshinetskiy, I. M., Samokhin, A. V., & Tsvetkov, Y. V. 2015. Fabrication of coatings on the surface of magnesium alloy by plasma electrolytic oxidation using ZrO_2 and SiO_2 nanoparticles. *Journal of Nanomaterials, 2015*.

77 Imshinetskiy, I. M., Gnedenkov, S. V., Sinebryukhov, S. L., Mashtalyar, D. V., Samokhin, A. V., & Tsvetkov, Y. V. 2014. Incorporation of zirconia and silica nanoparticles into PEO-coatings on magnesium alloys. *Solid State Phenomena, 213*, 125–130.

78 Lu, X., Chen, Y., Blawert, C., Li, Y., Zhang, T., Wang, F., ... & Zheludkevich, M. 2018. Influence of SiO2 particles on the corrosion and wear resistance of plasma electrolytic oxidation-coated AM50 Mg alloy. *Coatings, 8*(9), 306.

79 Xu, G., & Shen, X. 2019. Fabrication of SiO_2 nanoparticles incorporated coating onto titanium substrates by the micro arc oxidation to improve the wear resistance. *Surface and Coatings Technology, 364*, 180–186.

80 Tian, P., Liu, X., & Ding, C. 2015. In vitro degradation behavior and cytocompatibility of biodegradable AZ31 alloy with PEO/HT composite coating. *Colloids and Surfaces B: Biointerfaces, 128*, 44–54.

81 Mingo, B., et al. 2018. Influence of sealing post-treatments on the corrosion resistance of PEO coated AZ91 magnesium alloy. *Applied Surface Science, 433*, 653–667.

82 Zeng, D., Liu, Z., Bai, S., & Wang, J. 2019. Influence of sealing treatment on the corrosion resistance of PEO coated Al-Zn-Mg-Cu alloy in various environments. *Coatings, 9*(12).

83 Park, J., Seo, E., Lee, M., & Kim, D. 2022. Fabrication of a CuO composite PEO and effect of post-treatment on improving its thermal properties and corrosion resistance of magnesium alloy AZ31. *Surface and Coatings Technology, 447*, 128828.

84 Fakhr Nabavi, H., & Aliofkhazraei, M. 2019. Morphology, composition and electrochemical properties of bioactive-TiO_2/HA on CP-Ti and Ti6Al4V substrates fabricated by alkali treatment of hybrid plasma electrolytic oxidation process (estimation of porosity from EIS results). *Surface and Coatings Technology, 375*, 266–291.

85 Liu, C., Lu, X., Li, Y., Chen, Q., Zhang, T., & Wang, F. 2021. Influence of post-treatment process on corrosion and wear properties of PEO coatings on AM50 Mg alloy. *Journal of Alloys and Compounds, 870*, 159462.

86 Joseph, J., Gallo, S. C., Catubig, R., Wang, K., Somers, A., Howlett, P., & Fabijanic, D. 2020. Formation of a corrosion-resistant coating on zinc by a duplex plasma electrolytic oxidation and conversion surface treatment. *Surface and Coatings Technology, 395*, 125918.

87 Wang, S., Wang, Y., Cao, G., Chen, J., Zou, Y., Yang, B., ... & Zhou, Y. 2021. Highly reliable double-layer coatings on magnesium alloy surfaces for robust superhydrophobicity, chemical durability and electrical property. *Ceramics International, 47*(24), 35037-35047.

88 Mehri Ghahfarokhi, N., Shayegh Broujeny, B., Hakimizad, A., & Doostmohammadi, A. 2022. Plasma electrolytic oxidation (PEO) coating to enhance in vitro corrosion resistance of AZ91 magnesium alloy coated with polydimethylsiloxane (PDMS). *Applied Physics A: Materials Science and Processing, 128*(2), 1–13.

89 Toorani, M., Aliofkhazraei, M., Mahdavian, M., & Naderi, R. 2021. Superior corrosion protection and adhesion strength of epoxy coating applied on AZ31 magnesium alloy pre-treated by PEO/Silane with inorganic and organic corrosion inhibitors. *Corrosion Science, 178*, 109065.

90 Parichehr, R., Dehghanian, C., & Nikbakht, A. 2021. Preparation of PEO/silane composite coating on AZ31 magnesium alloy and investigation of its properties. *Journal of Alloys and Compounds, 876*, 159995.

91 Wierzbicka, E. 2021. Flash-PEO as an alternative to chromate conversion coatings for corrosion protection of Mg alloy.

92 Malayoglu, U., Tekin, K. C., & Shrestha, S. 2010. Influence of post-treatment on the corrosion resistance of PEO coated AM50B and AM60B Mg alloys. *Surface and Coatings Technology, 205*(6), 1793-1798.

93 Laleh, M., Kargar, F., & Sabour Rouhaghdam, A. 2011. Improvement in corrosion resistance of micro arc oxidation coating formed on AZ91D magnesium alloy via applying a nano-crystalline sol-gel layer. *Journal of Sol-Gel Science and Technology, 59*(2), 297–303.

94 Anawati, H., Asoh, H., & Ono, S. 2015. Enhanced uniformity of apatite coating on a PEO film formed on AZ31 Mg alloy by an alkali pretreatment. *Surface and Coatings Technology, 272*, 182–189.